Fe-V Sulfur Clusters studied through Photoelectron Spectroscopy and Density Functional Theory

Journal:	*Physical Chemistry Chemical Physics*
Manuscript ID	CP-ART-05-2018-003157.R2
Article Type:	Paper
Date Submitted by the Author:	31-Jul-2018
Complete List of Authors:	Yin, Shi; Colorado State University, Department of Chemistry, Bernstein, Elliot; Colorado State University, Department of Chemistry

Fe-V Sulfur Clusters studied through Photoelectron Spectroscopy and Density Functional Theory

*Shi Yin, Elliot R. Bernstein**

Department of Chemistry, NSF ERC for Extreme Ultraviolet Science and Technology, Colorado State University, Fort Collins, CO 80523, USA

AUTHOR INFORMATION

Corresponding Author

*Elliot R. Bernstein, E-mail: erb@lamar.colostate.edu.

ABSTRACT

Iron-vanadium sulfur cluster anions are studied by photoelectron spectroscopy (PES) at 3.492 eV (355 nm) and 4.661 eV (266 nm) photon energies, and by Density Functional Theory (DFT) calculations. The structural properties, relative energies of different structural isomers, and the first calculated vertical detachment energies (VDEs) of different structural isomers for cluster anions $FeVS_{1-3}^-$ and $Fe_mV_nS_{m+n}^-$ ($m + n = 3, 4$; $m > 0$, $n > 0$) are investigated at a BPW91/TZVP theory level. The experimental first VDEs for these Fe-V sulfur clusters are reported. The most probable ground state structures and spin multiplicities for these clusters are tentatively assigned by comparing their theoretical and experiment first VDE values. For $FeVS_{1-3}^-$ clusters, their first VDEs are generally observed to increase with the number of sulfur atoms from 1.45 eV to 2.86 eV. The NBO/HOMOs of ground state of $FeVS_{1-3}^-$ clusters are localized in a *p* orbital on a S atom: the partial charge distribution on their NBO/HOMO localized

sites of each cluster anion is responsible for the trend of their first VDEs. A less negative localized charge distribution is correlated with a higher first VDE. Structure and steric effect differences for $Fe_mV_nS_{m+n}^-$ ($m + n = 3$, $m > 0$, $n > 0$) clusters are suggested to be responsible for their different first VDEs and properties. Two types structural isomers are identified for $Fe_mV_nS_{m+n}^-$ ($m + n = 4$, $m > 0$, $n > 0$) clusters: a tower structure isomer and a cubic structure isomer. The first VDEs for tower like isomers are generally higher than those for cubic like isomers of $Fe_mV_nS_{m+n}^-$ ($m + n = 4$, $m > 0$, $n > 0$) clusters. Their first VDEs are can be understood through: (1) NBO/HOMO distributions, (2) structures (steric effect), and (3) partial charge number on the NBO/HOMO's localized sites. EBEs for excited state transitions for all Fe-V sulfur clusters are calculated employing OVGF and TDDFT approaches at the TZVP level. The OVGF approach for these Fe/V/S cluster anions is better for the higher transition energies than the TDDTF approach. The experimental and theoretical results for these Fe/V/S cluster anions are compared with their related pure iron sulfur cluster anions. Properties of the NBO/HOMO are essential for understanding and estimating the different first VDEs for Fe/V/S, and comparing them to those of the pure Fe/S cluster anions.

INTRODUCTION

Iron sulfur clusters are prevalent in both biological and industrial systems, [1-7] as has been recognized for many decades. Investigations of iron–sulfur systems, ranging from bare Fe–S clusters to analogue complexes and proteins, are common throughout bioinorganic chemistry. Synthesis and characterization of iron sulfur clusters and complexes comprise a large sub-field of organometallic chemistry. [8] A number of studies have been performed on gas phase cationic, [9, 10] neutral, [11, 12] and anionic [13-20] iron sulfur clusters for investigation of their composition, stability, structure, and reactivity. Extensive theoretical efforts devoted to the structural evolution of electronic properties of iron-sulfur complexes have also appeared. [21-25] For example, the structure of $Fe_2S_2^-$ cluster is assigned to be a planar rhomboid, the structure of $Fe_3S_3^-$ cluster is assigned to be a planar six-member ring, and a cubic structure is assigned for the $Fe_4S_4^-$ cluster. [26]

Trace elements, such as vanadium, are found to be essential for both biological and general catalytic systems. [27-33] The bacterial enzyme nitrogenase can catalyze the reduction of atmospheric N_2 to NH_3 and is responsible for cycling about 108 tons of N per year from the atmosphere to the soil. [29] Modeling the enzymatic N_2 fixation process remains one of the great challenges for bioinorganic chemists. Many studies find that Fe-V

mixed metal sulfur clusters in enzymes can be characterized as an active catalytic site; for example, an Fe/V/S anionic cluster is suggested to be responsible for the conversion of N_2 to NH_3. [33] Therefore, investigations of iron–vanadium mixed metal sulfur systems, ranging from small Fe–V sulfur clusters to analogous complexes and proteins, are common throughout bioinorganic chemistry.

Photoelectron spectroscopy (PES) has been proven to be a successful approach for study of electronic and geometric structures of atomic and molecular clusters, [35] as it combines size selectivity with spectral sensitivity and can generate information on both ionic and neutral species. These gas phase experimental results can then be directly and accurately compared to the calculated ones for the clusters of interest. [13] Computational chemistry has a very important role to play in helping to predict and rationalize the nature of the electronic ground state of transition metal compounds. [36] PES experimental results for cluster anions are also essential as tests for the performance of appropriate computational and theoretical methods. Electron binding energy of Fe-V sulfur clusters obtained from theory can be compared with those obtained from experiment to justify the theoretical method. Theoretical results obtained by provably reliable calculations can then be employed to analyze further PES spectra and finally generate

geometric and electronic structures for those Fe-V sulfur clusters that are not directly observable experimentally. Thus, theoretical calculations for both anionic and neutral systems can be employed to explore cationic species, as well.

This report presents a PES study of a series of Fe-V mixed metal sulfur cluster anions, employing a magnetic-bottle time-of-flight (MBTOF) photoelectron spectroscopy (PES) apparatus. The PES spectra of these cluster anions at 355 nm and 266 nm photon energies are reported, and the structural and electronic properties of these cluster anions are investigated by density functional theory (DFT). The most probable ground state structures and spin multiplicities of this small, neutral, and anionic cluster series are thereby assigned by comparing the theoretical first vertical detachment energies (VDEs) with their experiment values.

METHODS

A. Experimental

The MBTOF-PES experimental setup, consisting of a laser vaporization cluster/molecular source, an orthogonal acceleration/extraction reflectron time of flight (oaRETOF) mass spectrometer (MS), a mass gate, a momentum decelerator, and a MBTOF electron analyzer, employed in this work has been described previously in detail. [37, 38] Only a brief outline of the

apparatus is given below. In this work, Fe/V/S clusters are generated by laser ablation of a mixed iron/vanadium target [made by pressing a mixture of iron (99.9%, Sigma Aldrich) and vanadium (99.9%, Sigma Aldrich) powders with a ratio of Fe:V = 1:1] in the presence of a 0.1 % CS_2 in helium carrier gas. A 10 Hz, focused, 532 nm Nd^{3+}:YAG (Nd^{3+}: yttrium aluminum garnet) laser with ~ 5 mJ/pulse energy is used for the laser ablation. The expansion gas is pulsed into the vacuum by a supersonic nozzle (R. M. Jordan, Co.) with a backing pressure of typically 100 psi. The mass spectrum obtained from above generation methods are given as Figure S1 in the Supporting Information. The ablation laser energy is adjusted from 1 to 10 mJ/pulse to seek the best generation condition for Fe-V sulfur clusters. The intensity of mass spectral features for $Fe_mV_nS_x^-$ cluster anions is observed to be related to ablation laser energy. The intensity of mass spectrum increases when ablation laser energy is adjusted from 1 to ~ 5 mJ/pulse, and then decreases if ablation laser energy keeps increasing from 5 to 10 mJ/pulse. This behavior suggests that the obtained MS and PES profiles are probably affected by cluster source conditions. The mass selected and decelerated anions are exposed to different laser wavelengths (355 nm, 266 nm) at the photo-detachment region. The photo-detached electrons are energy analyzed by the MBTOF-PES spectrometer. PES spectra are collected and calibrated

at this resolution with known spectra of Cu^-. [39]

B. Theoretical

All calculations are performed using the Gaussian 09 program package. [40] The structures of Fe/V/S clusters are optimized for different isomers and spin multiplicities using DFT without constraints. For each cluster, different initial structures are employed as input in the optimization procedure. There are many possible structures, especially for the lager clusters. Unfortunately, we are probably not able to calculate all possibilities, but an extensive search for the global minimum structure has been pursued for each cluster: for example, see calculated structures of $FeV_3S_4^-$ cluster in Figure S2 in the supporting information, SI. The magnetic (spin) properties of iron containing clusters stand as their most fundamental characteristic and thereby provide an indispensable and essential means for their characterization. Therefore, spin-dependent delocalization, depicting ferromagnetic and antiferromagnetic spin alignments, is one of the most interesting, essential, and challenging topics for iron containing cluster studies. [24, 41, 42] In this work, the relative energies for each cluster with different spin multiplicities ((M = (2S + 1)) from low to high are investigated at the BPW91/TZVP level. Broken-symmetry is employed for low spin calculations (see details in the Supporting Information). Generally, the lowest relative energy spin state is

selected and discussed for each structure isomer of small $Fe_mV_nS_x^-$ ($m + n$ = 2, 3) clusters. For larger $Fe_mV_nS_x^-$ ($m + n = 4$) clusters, several spin states are found to be relative energy degenerate and lowest, so these spin states are all discussed in Section C below. In our previous studies of iron sulfur clusters, [26] the spin-orbit coupling (SOC) corrections are found insignificant for the calculations of relative energies of the spin states and the first VDE of small clusters, such as $(FeS)_{1,2}^-$ (details are given in the Supporting Information). Thus, SOC corrections are neglected for calculations of relative energies of the spin states and the first VDEs of Fe-V sulfur clusters studied in this work at the present level of theory. Nonetheless, SOC may be important for larger clusters, however, which present a symmetrical environment for iron centers. [43] All relative energies are zero point energy corrected. Vibrational frequency calculations are further performed to confirm global minima, which have zero imaginary frequency. The Perdew–Wang [44] correlation functional (BPW91) combined with the triple-ζ valence plus polarization (TZVP) [45] basis sets, which are proved to have good performance in previous studies of iron sulfur [12, 37] and vanadium sulfur clusters, [46] are employed to explore these Fe/V/S clusters. In our previous studies of iron sulfur and vanadium sulfur clusters, different reasonable functionals (B3LYP, [47, 48] B3PW91, [49, 50] and APFD [51]) and basis sets (6-311+G(d) [52-54]) are employed to calculate the

relative energy and the first VDE of the studied clusters (such as $(FeS)_4^-$ [26]) with different spin multiplicities. The basis set aug-cc-PV5Z [55] for sulfur atoms and TZVP for iron atoms are also employed and tested to seek a more secure assignment. All above calculation methods are selected for comparison with BPW91/TZVP level calculations to ensure that the latter method is sufficient to explore description of iron sulfur anion clusters studied by us previously. Calculated results for relative energy (ΔE) and the first VDE of studied clusters with different spin multiplicity employing different functionals and basis sets are indistinguishable from one another and consistent with the experimental results (VDEs). [26] Such comparisons make clear that the performance of BPW91/TZVP is more than sufficient for investigation of Fe-V sulfur clusters, so the method BPW91/TZVP is adopted for the present studies. All calculations are treated in a spin-unrestricted manner.

In this approach, for each spin state of the Fe-V sulfur cluster anion, the first vertical detachment energy (VDE = $E_{\textit{neutral at optimized anion geometry}} - E_{\textit{optimized anion}}$) is calculated as the lowest transition from the spin state (M) of the anion into the spin state ($M + 1$ *or* $M - 1$, $M = 2S + 1$) of the related neutral species at the geometry optimized for the anion. The $M + 1$ spin state of the related neutral species is considered for the process, in which the photo detached

electron comes from paired electrons, and the $M - 1$ spin state of the related neutral species is considered as that the photo detached electron comes from an unpaired electron. The other spin states of the related neutral species are not considered, because a second electron transition or spin conversion process must be considered for such a transition. Compared with the transition of M spin state ion to $M + 1$ *or* $M - 1$ spin states of the related neutral species, a second electron transition or spin conversion process in the related neutral species should have significantly lower probability (intensity). The optimized anion geometries are used for the further calculations of the photoelectron spectra employing time-dependent density functional theory (TDDFT). [56] Vertical excitation energies of the neutral species are added to the first VDE of the relative Fe-V sulfur anion clusters to obtain their second and higher EBEs. The outer valence Green function method (OVGF/TZVP) [57] is also used to calculate the second and higher VDEs of these Fe-V sulfur anion clusters.

An NBO analysis is an often employed orbital (wave function) localization and population analysis method to help understand the electron distribution in a molecule or cluster around particular sites or moieties of interest. Within this method, natural atomic orbitals (NAOs), determined for the particular species under consideration, are evaluated and employed: NAOs are the

effective orbitals of an atom in the particular molecular environment (rather than for isolated atoms). NAOs are also the maximum occupancy orbitals. Information obtained from an NBO analysis, such as partial charges and HOMO-LUMO orbitals, is reported to explain, for example, a number of experimental phenomena of gas phase 1-butyl-3-methylimidazolium chloride ion pairs. [58] The NBO calculations in this work are performed using the NBO 3.1 program as implemented in the Gaussian 09 package. Partial charge distributions of cluster anions studied in this work are calculated using NBO analysis.

RESULTS AND DISCUSSION

A. Studies of the $FeVS_{1-3}^-$ cluster anions.

Photoelectron Spectra of $FeVS_{1-3}^-$.

The obtained PE spectra for the $FeVS_{1-3}^-$ cluster anions at different photon energies are shown in Figure 1. Photo detachment transitions occur between the ground state of an anion and the ground and excited states of its neutral counterpart, at the structure of the anion. The profile of the transition is governed by the Franck–Condon overlap between the two species, the anion and the neutral. The electron binding energy (EBE) value at the intensity maximum in the Franck–Condon profile is the vertical detachment energy (VDE). The first VDE, proving important in establishing a cluster's

electronic and geometric structure, is derived from the energy of the first peak maxima in the photoelectron spectra. As the PE spectra of $FeVS^-$ cluster shown in Figure 1a and 1b, two features are observed at both 355 nm and 266 nm, and their measured VDEs are 1.45 (X) and 2.85 (A) eV, respectively. In Figure 1c, two features are observed in the PE spectrum of $FeVS_2^-$ cluster at 355 nm, and their measured VDEs are 1.63 (X') and 2.55 (X) eV. Two peaks are observed for the higher transition labeled feature A (3.45 eV) and B (4.20 eV) at 266 nm photon energy (Figure 1d). For the PE spectrum obtained for $FeVS_3^-$ cluster (Figure 1e), only one peak (2.86 eV, X) is observed at 355 nm. The second peak is observed for the higher transition labeled feature A (3.65 eV) at 266 nm photon energy (Figure 1f).

DFT calculations for $FeVS_{1-3}^-$.

Determination of the geometrical structures of the clusters is important, since this cluster property is the basis for the description of all other cluster characteristics (e.g., electronic structure, electron density, charge and spin densities, etc.). Various structural isomers of Fe-V sulfur clusters discussed in this work are investigated, and different spin multiplicities from low to high are considered for each isomer. The relative energy differences (ΔE, ΔG) between different structural isomers with different spin multiplicities are calculated and compared to evaluate their relative stability. The structure and

spin multiplicity for the ground state of a cluster anion is assigned mainly based on agreement of the calculated first VDEs compared to the experimental values. The calculated VDEs (in eV) for $FeVS_{1-3}^-$ clusters at BPW91/TZVP level, as well as the experimental results for comparison are shown in Table I.

Three types structural isomers are obtained from calculations for the $FeVS^-$ cluster anion. Structural details of the three isomers are displayed in Figure 2a. Comparing their calculated first VDEs with the experimental values obtained in Figure 1a, 1b, and Table I, the calculated VDEs of isomer I (1.82 eV) and isomer III (1.61 eV) of $FeVS^-$ are both in reasonable agreement with the experimental value of the X labeled feature (1.45 eV). These results suggest both structural isomers I and III of $FeVS^-$ probably exist under the experimental conditions and contribute to the PE spectrum for the $FeVS^-$ cluster, but structural isomer II of $FeVS^-$ probably does not exist in the anion beam. Comparison of PES experimental VDEs to calculated ones is the appropriate method by which to study and assign the actual structures and properties of the clusters present.

Two types structural isomers are obtained theoretically for the $FeVS_2^-$ cluster anion: the geometric details of isomers I and II are displayed in Figure 2b. Isomer I of $FeVS_2^-$ has one terminal sulfur bonded to a vanadium site, and

isomer II of $FeVS_2^-$ has a four-member ring structure. Comparing their calculated first VDEs with the experimental values obtained in Figure 1c, 1d, and Table I, the calculated VDE of isomer I (2.46 eV) of $FeVS_2^-$ is in good agreement with the experimental value of the X labeled feature (2.55 eV), and the calculated VDE of isomer II (1.76 eV) of $FeVS_2^-$ is also in good agreement with the experimental value of the X' labeled feature (1.63 eV).

For $FeVS_3^-$ cluster anion, three types structural isomer are obtained theoretically and their geometric details are displayed in Figure 2c. Comparing their calculated first VDEs with the experimental values obtained in Figure 1e, 1f, and Table I, the calculated first VDE of isomers I (2.46 eV), II (2.87 eV), and III (2.76 eV) of $FeVS_3^-$ are close (within ~ 0.4 eV), and are all in good agreement with the experimental value of the X labeled feature (2.86 eV). These results suggest structural isomers I, II, and III of $FeVS_3^-$ probably all exist under the experimental conditions and contribute to the PE spectrum for $FeVS_3^-$ cluster.

In sum, the experimental first VDEs are generally observed to increase with the number of sulfur atoms from 1.45 eV to 2.85 eV for these $FeVS_{1-3}^-$ clusters. Diverse types of structural isomers are found for each $FeVS_x^-$ (x = 1 – 3) cluster. One type of structural isomer with a terminal sulfur bonded to a vanadium site (isomer I) is found for all $FeVS_{1-3}^-$ clusters, and its calculated

relative energy (ΔE) is obtained to be the lowest among all structural isomers for each species $FeVS_x^-$ ($x = 1 – 3$).

Understanding the first VDEs for $FeVS_{1-3}^-$ through structure, NBO/HOMO distribution, and partial charge distribution.

To estimate the first VDEs of cluster anions, one electron is removed from the highest occupied molecular orbital (HOMO) of the cluster maintaining the cluster optimized geometry. Therefore, studies of HOMO properties of these $FeVS_{1-3}^-$ clusters are helpful to understand their different first VDEs. Furthermore, partial atomic charges are suggested to play a decisive role in determining core electron binding energy in small molecules. [59] The partial charge at the HOMO localized site in these Fe-V sulfur cluster anions may to some extent affect the energy (first VDE) required to remove an electron from such clusters through a "charge effect". A small negative charge number at the site means less electron density distribution on that site (i.e., site is more positive than anticipated), and therefore removal of an electron from that site may require more energy than otherwise estimated based simply on the NBO/HOMO distribution for that site. In order to investigate and understand the above interesting physical behavior for $FeVS_{1-3}^-$ clusters, NBOs and NBO charges for each atom are calculated for all assigned ground state isomers: isomers I of $FeVS_{1,3}^-$ cluster anions, and isomers I and II of

$FeVS_2^-$ clusters anions. For the latter case, both features X' and X are identified.

Electron density distribution plots for $FeVS_{1-3}^-$ cluster NBO/HOMOs are shown in Figure 3. The experimental first VDEs of $FeVS_{1-3}^-$ clusters increase with the number of sulfur atoms: from 1.45 eV of $FeVS^-$, to 2.55 eV of $FeVS_2^-$, and to 2.86 eV of $FeVS_3^-$. The NBO/HOMOs of all isomers I of $FeVS_{1-3}^-$ present major electron distribution similar to that of localized *p* orbitals on the terminal S atom. The NBO partial charge numbers of the S sites, on which the NBO/HOMO is localized, are -0.871 for isomer I of $FeVS^-$, -0.560 for isomer I of $FeVS_2^-$, and -0.309 for isomer I of $FeVS_3^-$ (see Figure 3). Since the S atom is more electronegative than iron or vanadium atoms, the negative charge number at the S site in these Fe-V sulfur clusters is not unreasonable. The observed increase of the first VDE for these $FeVS_{1-3}^-$ clusters with the number of sulfur atoms is consistent with the decrease negative charge number of their NBO/HOMO localized S site. These results suggest that above proposed "charge effect" is probably an important factor responsible for the trend of the first VDEs of these ground state (isomer I) $FeVS_{1-3}^-$ cluster anions.

B. Studies of the $Fe_mV_nS_{m+n}^-$ ($m + n = 3$, $m > 0$, $n > 0$) cluster anions.

Photoelectron Spectra of $Fe_mV_nS_{m+n}^-$ ($m + n = 3$, $m > 0$, $n > 0$).

The obtained PE spectra for the $Fe_mV_nS_{m+n}^-$ ($m + n = 3$, $m > 0$, $n > 0$) cluster anions at different photon energies are shown in Figure 4. As the PE spectrum of $FeV_2S_3^-$ cluster shown in Figure 4a, one broad feature (X) is observed at 355 nm, and its measured first VDE is 2.00 eV. Another broad peak is observed for the higher transition labeled feature A (3.17 eV) at 266 nm photon energy (Figure 4b). In the PE spectra of $Fe_2VS_3^-$ cluster, one peak (3.18 eV, X) is partly observed at 355 nm (Figure 4c), and the second peak is observed for the higher transition labeled feature A (~ 4.0 eV) at 266 nm photon energy (Figure 4d).

DFT calculations for $Fe_mV_nS_{m+n}^-$ ($m + n = 3$, $m > 0$, $n > 0$).

Calculated VDEs (in eV) for $FeV_2S_3^-$ and $Fe_2VS_3^-$ clusters at the BPW91/TZVP level, as well as the experimental results for comparison are shown in Table II. Two types structural isomers are obtained calculationally for the $FeV_2S_3^-$ cluster anion; the geometric details are displayed in Figure 5a. Comparing their calculated first VDEs with the experimental values obtained in Figure 4a, 4b, and Table II, the calculated VDE for isomer II (2.22 eV) of $FeV_2S_3^-$ is in slightly better agreement with the experimental value of the X labeled feature (2.00 eV) than that for isomer I (2.55 eV) of $FeV_2S_3^-$.

For the $Fe_2VS_3^-$ cluster anion, two types structural isomer are also obtained

theoretically: geometric details for isomers I and II are displayed in Figure 5b. As presented in Table II, the calculated VDE of isomer I of $Fe_2VS_3^-$ is 2.58 eV, which is similar to the experimental value 3.18 eV obtained from the X labeled feature in Figure 4c and 4d.

Understanding the first VDEs for $Fe_mV_nS_{m+n}^-$ ($m + n = 3$, $m > 0$, $n > 0$) through structure, NBO/HOMO distribution, and partial charge distribution.

Due to comparison of calculated VDEs with experimental values as discussed above, the ground state of the $Fe_2VS_3^-$ cluster anion is assigned to be isomer I, whose structure is a planar six-member ring as shown in Figure 5b. The ground state of the $FeV_2S_3^-$ cluster anion is assigned to be isomer II, whose structure is 3-dimensional as shown in Figure 5b. The experimental first VDEs for the above three metal, three sulfur $FeV_2S_3^-$ and $Fe_2VS_3^-$ clusters, are about one eV different. The experimental first VDE of $Fe_2VS_3^-$ (3.18 eV) is ~ 1.2 eV higher than that of $FeV_2S_3^-$ (2.00 eV) as displayed in Table II. With the same analysis strategy used above in Section A for two metal atoms containing $FeVS_{1-3}^-$ clusters, NBOs and NBO partial charges for each atom are calculated for both assigned ground state isomers (II) of $FeV_2S_3^-$ and (I) of $Fe_2VS_3^-$ clusters anions to understand their different properties.

As plots of distributions for their NBO/HOMOs show in Figure 6, NBO/HOMOs of both isomers present major electron distribution similar to that of localized *p* orbitals on a S atom. The NBO partial charge numbers of the S sites, on which the NBO/HOMO is localized, are -0.468 for isomer II of $FeV_2S_3^-$, and -0.638 for isomer I of $Fe_2VS_3^-$. Note that, the charge number for the NBO/HOMO localized site of isomer II of $Fe_2VS_3^-$ is more negative than that of isomer I of $FeV_2S_3^-$, but the first VDE for $Fe_2VS_3^-$ (3.18 eV) is higher than that of $FeV_2S_3^-$ (2.00 eV). These results suggest the "charge effect" proposed in section A is not the only factor to affect the first VDEs of these large three metal containing Fe-V sulfur cluster anions. For the 3-dimensional structural isomer II of $FeV_2S_3^-$, the NBO/HOMO localized sulfur atom bonds with two vanadium atoms, and that < VSV angle is 47.78° (Figure 5a and 6). For the planar structural isomer I of $Fe_2VS_3^-$, the NBO/HOMO localized sulfur atom bonds with two iron atoms, and that < FeSFe angle is 62.77° (see Figure 5b and 6). Their structures are different, and that bigger metal – sulfur (NBO/HOMO localized) – metal angle (62.77°) for isomer I of $Fe_2VS_3^-$ means a larger steric effect for the electron detachment than those for isomer II of $FeV_2S_3^-$. This structure and steric effect difference between $FeV_2S_3^-$ and $Fe_2VS_3^-$ clusters probably is responsible to their different first VDEs.

In sum, three metal atoms containing Fe/V/S anions, $FeV_2S_3^-$ and $Fe_2VS_3^-$ clusters, are discussed in this section through PES and DFT. The first VDE for $Fe_2VS_3^-$ is observed ~ 1.2 eV higher than that of $FeV_2S_3^-$. Their NBOs are found to be the same and localize on S atom *p* orbitals. The "charge effect" for the NBO/HOMO localized site is not suggested to be a major factor affecting their first VDEs. With different Fe/V ratios, their ground state structures are assigned to be different, and their structure and steric effect difference are suggested to be responsible for their different first VDEs and properties. Note that, the structures of ground state $FeVS_{1-3}^-$ clusters discussed in Section A are simpler (all close to planar) than these three metal atoms containing Fe-V sulfur ($FeV_2S_3^-$ and $Fe_2VS_3^-$) clusters: the trend of the first VDEs of $FeVS_{1-3}^-$ cluster anions can be rationalized by a "charge effect" at their comparable NBO/HOMO localized sites. Therefore, structure apparently plays a more important role for the properties of these Fe-V mixed sulfur cluster as their size increases: this correlation is especially important for understanding and estimating their first VDEs.

C. Studies of $Fe_mV_nS_{m+n}^-$ ($m + n = 4$, $m > 0$, $n > 0$) cluster anions.

Photoelectron Spectra of $Fe_mV_nS_{m+n}^-$ ($m + n = 4$, $m > 0$, $n > 0$).

In this section, four metal atom containing Fe-V sulfur clusters $Fe_mV_nS_{m+n}^-$ ($m + n = 4$, $m > 0$, $n > 0$) are discussed. Their PE spectra are shown in

Figure 7. The PE spectrum of the $FeV_3S_4^-$ cluster shown in Figure 7a, evidences one broad feature at 355 nm excitation: its measured first VDE is ~ 2.7 (X) eV. Another broad peak is observed for the higher transition labeled feature A (~ 4.0 eV) at 266 nm photon energy (Figure 7b). In Figure 7c, two features are observed in the PE spectrum of the $Fe_2V_2S_4^-$ cluster at 355 nm: their measured VDEs are 1.50 (X') and 2.17 (X) eV. One broad peak is observed for the higher transition labeled feature A (~ 3.5 eV) obtained at 266 nm photon energy (Figure 7d). For the $Fe_3VS_4^-$ cluster anion, only broad peaks are observed (Figure 7f). The first peak (X'') is around 1.60 eV, and the second peak (X') is around 2.3 eV. Another feature labeled X is observed at 3.20 eV. At higher binding energy, a broad peak (A) is detected from 3.5 eV to 4.4 eV.

DFT calculations for $Fe_mV_nS_{m+n}^-$ ($m + n = 4$, $m > 0$, $n > 0$)

Calculated VDEs (in eV) for $Fe_mV_nS_{m+n}^-$ ($m + n = 4$, $m > 0$, $n > 0$) cluster anions at the BPW91/TZVP level, as well as experimental results for comparison, are presented in Table III. Two types structural isomers are obtained from these calculations for each $FeV_3S_4^-$, $Fe_2V_2S_4^-$, and $Fe_3VS_4^-$ cluster anion. Isomer I of each $Fe_mV_nS_{m+n}^-$ ($m + n = 4$, $m > 0$, $n > 0$) has a tower like structure and isomer II of each $Fe_mV_nS_{m+n}^-$ ($m + n = 4$, $m > 0$, n > 0) has a cubic like structure.

As displayed in Table III, the calculated first VDE for isomer I (2.64 eV) of $FeV_3S_4^-$ is in very good agreement with the experimental value of the X labeled feature (~ 2.7 eV).

For $Fe_2V_2S_4^-$ cluster anions, the two lowest relative energy (ΔE) spin states of each structural isomer are found to be degenerated (Table III). Note that the intensity of peak X' is lower than that of peak X in Figures 7c and 7d. The ΔE for isomer II of $Fe_2V_2S_4^-$ is ~ 0.4 eV higher than that for isomer I, which agrees with that intensity difference observation for X and X' peaks, considering that the higher ΔE implies a less stable state with a lower population. These results imply that both structural isomer I and II of $Fe_2V_2S_4^-$ exist under the experimental conditions and contribute to the PE spectrum for $Fe_2V_2S_4^-$ cluster anions, and that their multiple low ΔE spin states should also be considered when evaluating their properties and behavior in real chemical and biological systems.

The first VDEs and EBEs for both tower like structure isomer I and cubic like structure isomer II (see details in Figure 8c) of $Fe_3VS_4^-$ are also calculated and presented in Table III. From Figure 7f, intensity of peaks decreases in the order X, X', X''. This trend for $Fe_3VS_4^-$ clusters can be understood based on the increase of ΔEs for nonet isomer I (X feature) to 11-et isomer I (X' feature), and to nonet and 11-et isomer II (X'' feature). These

observations and comparisons illustrate that not only do the lowest relative energy spin state and isomer exist in the experimental system, but also that the relative populations of the diverse co-existing spin states and isomers may relate to their relative energies.

Important details for whether or not such relative energy populations and spectroscopic intensities are appropriately compared and related to one another are typically contained in the particular characteristics and cross over points associated with the potential energy surfaces (stationary points, barrier heights, and intermediates states) for the various isomers of each cluster anion.

Understanding the first VDEs for $Fe_mV_nS_{m+n}^-$ ($m + n = 4$, $m > 0$, $n > 0$) through structure, NBO/HOMO distribution, and partial charges.

From above results and discussion for four metal atom containing Fe-V sulfur clusters $Fe_mV_nS_{m+n}^-$ ($m + n = 4$, $m > 0$, $n > 0$), we find that the experimental VDEs for tower like structure isomers are generally higher than those for cubic like structure isomers of these $Fe_mV_nS_{m+n}^-$ ($m + n = 4$, $m > 0$, $n > 0$) clusters. To understand these results, NBOs and NBO partial charges for each atom are calculated for observed structural isomers of $Fe_mV_nS_{m+n}^-$ ($m + n = 4$, $m > 0$, $n > 0$) clusters (Figure 9).

Regarding $Fe_mV_nS_{m+n}^-$ ($m + n = 4$, $m > 0$, $n > 0$) cluster anion experimental

VDEs, the following comparison consequences are obtained. First, the experimental VDE for tower like structure isomer I of $Fe_3VS_4^-$ is the highest, 3.20 eV. Its NBO/HOMO presents electron distribution similar to that of localized *p* orbitals on an S atom. The NBO partial charge number on its NBO/HOMO localized S site is -0.299. Second, for the other two tower like structure isomers, the experimental VDE for isomer I of $FeV_3S_4^-$ is 2.70 eV, and for isomer I of $Fe_2V_2S_4^-$ is 2.17 eV. Their NBO/HOMOs both present electron distribution similar to that of localized *d* orbitals on V atoms. The NBO partial charge number on their NBO/HOMOs localized V sites are positive, 0.192 (isomer I of $FeV_3S_4^-$) and 0.196 (isomer I of $Fe_2V_2S_4^-$). Third, for cubic like structure isomers, the experimental VDE for isomer II of $Fe_3VS_4^-$ is 1.60 eV, and for isomer II of $Fe_2V_2S_4^-$ is 1.50 eV. Their NBO/HOMOs also present electron distribution similar to that of localized *d* orbitals on V atoms. The NBO partial charge number on the their NBO/HOMOs localized V sites are negative, -0.281 (isomer II of $Fe_3VS_4^-$) and -0.075 (isomer II of $Fe_2V_2S_4^-$).

The above three comparisons suggest that more complex factors affect the electronic properties (the first VDEs) simultaneously for these four metal atoms containing Fe-V sulfur clusters $Fe_mV_nS_{m+n}^-$ ($m + n = 4$, $m > 0$, $n > 0$), instead of only one major factor. The structure with regard to steric effects,

NBO/HOMO distribution, and partial charge on the NBO/HOMO localized site (see the "charge effect" proposed in Section A) should all be considered to understand and estimate the changes of their first VDEs. The following three general rules can be derived based on the above results. First, NBO/HOMO distributions on S atoms compared to those on V atoms generate higher first VDE for the cluster, due to the higher electronegativity of S than that of V (Pauling electronegativity of S is 2.58, and of V is 1.63). This may be the reason that the highest first VDE (3.20 eV) observed for all $Fe_mV_nS_{m+n}^-$ ($m + n = 4$, $m > 0$, $n > 0$) cluster anions is isomer I of $Fe_3VS_4^-$ (NBO/HOMO distribution on S atom). Second, the tower structure tends to have a higher first VDE than the cubic structure due to its relatively strong steric effect. For example, NBO/HOMOs for both isomer I (tower like structure) and isomer II (cubic like structure) of $Fe_2V_2S_4^-$ are localized on *d* orbital V atoms. The larger S-V (NBO/HOMO localized)-S angle for isomer I (165.58°) than that for isomer II (~ 110.30°) implies a stronger steric effect for the tower structural isomer I of $Fe_2V_2S_4^-$. This structural effect is perhaps responsible for the higher first VDE for isomer I (2.17 eV) than that for isomer II (1.50 eV) of $Fe_2V_2S_4^-$. Third, the proposed "charge effect" still applies for these four metal atoms Fe-V sulfur clusters: the positive NBO partial charge numbers on the NBO/HOMOs localized V sites of $FeV_3S_4^-$

isomer I and $Fe_2V_2S_4^-$ isomer I may play a role in their higher first VDEs, as compared to the negative NBO partial charge numbers for the NBO/HOMOs localized V sites of $Fe_3VS_4^-$ isomer II and $Fe_2V_2S_4^-$ isomer II.

In sum, four metal atom containing Fe-V sulfur clusters $Fe_mV_nS_{m+n}^-$ ($m + n = 4$, $m > 0$, $n > 0$) cluster anions are analyzed in this section through PES and DFT. Two types of structural isomers (tower like and cubic like) are observed for $Fe_2V_2S_4^-$ and $Fe_3VS_4^-$ clusters; only tower like structural isomers are observed for the $FeV_3S_4^-$ cluster anions in the PES experiments. This suggests that the ratio of Fe and V atoms can affect the structure properties for these Fe-V sulfur clusters. The first VDEs of $Fe_mV_nS_{m+n}^-$ ($m + n = 4$, $m > 0$, $n > 0$) clusters are reported and suggested to be understood through three electronic properties: (1) NBO/HOMO distributions, (2) structures (steric effect), and (3) partial charge number on the NBO/HOMOs localized sites ("charge effect"). Note that comparisons of Tables 1-3 emphasize two distinct behaviors: 1. addition of metal atoms to these $Fe_mV_nS_{m+n}^-$ ($m + n = 2$-4, $m > 0$, $n > 0$) clusters does not affect their first VDEs systematically; and 2. addition of V or Fe atoms to these clusters also does not generate systematic changes for their first VDEs.

D. EBE values of low-lying transition peaks for $FeVS_{1-3}^-$ and $Fe_mV_nS_{m+n}^-$ ($m + n = 3, 4$; $m > 0$, $n > 0$) cluster anions

The electron binding energy (EBE) values, following the first VDE, are calculated employing TDDFT (BPW91/TZVP level) and OVGF/TZVP methods. The calculated results for $FeVS_{1-3}^-$ and $Fe_mV_nS_{m+n}^-$ ($m + n = 3, 4$; $m > 0$, $n > 0$) cluster anions are summarized and compared with their experimentally measured values in Table I to III, respectively.

EBEs regarding excited state transitions for related Fe/V/S are calculated employing OVGF and TDDFT approaches at a TZVP basis set level. The OVGF approach is found to be generally better for higher transition energy theoretical studies of $FeVS_{1-3}^-$, $Fe_2VS_3^-$, and $FeV_3S_4^-$ cluster anions, but not for $FeV_2S_3^-$. For $Fe_2V_2S_4^-$ and $Fe_3VS_4^-$ clusters, both approaches seem acceptable, mostly due to the breadth of the feature associated with their higher energy transition peaks. Therefore, both OVGF and TDDFT approaches are acceptable for these latter two cluster EBE calculations of Fe-V sulfur clusters regarding excited state transitions to obtain cautiously tentative assignments. The OVGF method may be preferred generally, however, due to its better agreement for most Fe-V sulfur clusters studied in this work.

E. Comparison of $Fe_mV_nS_{m+n}^-$ ($m + n = 2 - 4$, $m > 0$, $n > 0$) with pure $(FeS)_{2-4}^-$ cluster anions

Since pure iron sulfur clusters are also found to be important in biological

and industrial systems, comparing properties of the Fe-V sulfur clusters discussed above with properties of their related pure iron sulfur clusters becomes a useful endeavor.

As we reported previously, [26] $Fe_2S_2^-$ cluster anions have a four-member ring structure, which is similar to isomer II of $FeVS_2^-$. The NBO/HOMO of the $Fe_2S_2^-$ cluster is localized on a *p* orbital on a S atom, however, which is similar to the electronic NBO/HOMO of isomer I of $FeVS_2^-$. Interestingly, the experimental first VDE of $Fe_2S_2^-$ cluster is 2.34 eV, which is close to that of isomer I of $FeVS_2^-$ (2.55 eV), but not close to that of structures like isomer II of $FeVS_2^-$ (1.63 eV). This result suggests the electron distribution property of NBO/HOMO is a principal factor to be considered with regard to the first VDE of these small two metal containing metal sulfide clusters ($Fe_2S_2^-$ and $FeVS_2^-$).

Our previously reported experimental first VDE of the $Fe_3S_3^-$ cluster anion (3.57 eV) [26] is about ~ 0.4 and ~ 1.5 eV higher than those of the $Fe_2VS_3^-$ (3.18 eV) and $FeV_2S_3^-$ (2.00 eV) cluster anions. The NBO/HOMO of $Fe_3S_3^-$ clusters is delocalized as a Fe−Fe bonding orbital. Interestingly, the NBO/HOMOs of $FeV_2S_3^-$ (isomer II) and $Fe_2VS_3^-$ (isomer I) clusters both appear to be localized *p* orbitals on the S site; they are not observed localized on an Fe site. As proposed and discussed in the studies of

$(FeS)_mH_{0,1}$ (m = 2–4) cluster anions, the change of cluster VDE from low to high can be associated with the change in nature of their NBO/HOMO from a valence p orbital on S to an Fe–Fe delocalized valence bonding orbital. [60] Therefore, the distinctly different first VDEs of pure iron sulfur $Fe_3S_3^-$ and Fe-V sulfur $Fe_mV_{3-m}S_3^-$ (m = 1, 2) cluster anions can be related to the different NBO/HOMOs electron distribution (wave function) properties of each cluster anion.

The experimental first VDE for the $Fe_4S_4^-$ cluster previously reported [26] is 2.71 eV. The structure of this cluster anion is that of a distorted cube and its NBO/HOMO is that of a localized *d* orbital on an Fe site. Cubic like structures are also observed for $Fe_2V_2S_4^-$ and $Fe_3VS_4^-$ cluster anions. Their experimental first VDE are 1.50 eV, for $Fe_2V_2S_4^-$, and 1.60 eV for $Fe_3VS_4^-$; their NBO/HOMOs appear to be localized *d* orbital on the V sites. The lower first VDEs for these Fe-V sulfur clusters ($Fe_2V_2S_4^-$ and $Fe_3VS_4^-$) than those for $Fe_4S_4^-$ cluster anions may be related the smaller Pauling electronegativity for V (1.63) than that for Fe (1.83). These results also suggest that electron distribution of the NBO/HOMO is an essential characteristic through which one can understand and estimate the first VDEs of these big four metal containing metal sulfide cluster anions ($Fe_4S_4^-$, $Fe_2V_2S_4^-$ and $Fe_3VS_4^-$).

In sum, the structure evolution from Fe_2S_2 to Fe_4S_4 cluster is from planar

ring to three-dimensional cubic structures. [26] In this work, a similar trend is observed for Fe-V sulfur clusters $Fe_mV_nS_{m+n}^-$ ($m + n = 2 - 4$, $m > 0$, $n > 0$) with increased numbers of Fe and V atoms. A planar rhomboid structure is observed for the $FeVS_2^-$ (isomer II) cluster, planar six-member ring structures are found for both $Fe_2VS_3^-$ (isomer I) and $FeV_2S_3^-$ (isomer I) clusters, and cubic structures are assigned for four metal centers containing clusters $Fe_2V_2S_4^-$ (isomer II) and $Fe_3VS_4^-$ (isomer II). Other structural isomers are also observed/assigned for these V atoms involving clusters: for example, a planar structure containing a terminal S on V is also assigned for $FeVS_2^-$ (isomer I), a three-dimensional structure is only observed for $FeV_2S_3^-$ (isomer II), and tower like structures are found for all four metal centers containing $Fe_mV_nS_{m+n}^-$ ($m + n = 4$, $m > 0$, $n > 0$) clusters (isomer I). Note that the $FeV_3S_4^-$ cluster is only assigned as a tower like structure (isomer I). Compared to pure iron sulfur clusters, the Fe-V sulfur clusters have a more diverse set of structural isomers, probably due to the varied oxidation state properties of the V compared to those of Fe. The relative energy differences (ΔE) between different structural isomers with different spin multiplicities are calculated and compared to evaluate the relative stability of these Fe-V sulfur clusters. The structure and spin multiplicity for the ground state of a cluster anion is assigned mainly based on agreement of the calculated first

VDEs compared to the experimental values. Interestingly, the calculated first VDEs of all lowest ΔE structural isomers are in good agreement with the experimental value of studied Fe-V sulfur clusters, so the lowest ΔE structural isomer is generally assigned to be the ground state structure. Nonetheless, some structural isomers with high ΔE (less than 1 eV) are also observed in experiments, such as isomer II of $^{3}FeVS_2^-$ (ΔE = 0.32) and isomer II of $^{6}Fe_2V_2S_4^-$ (ΔE = 0.45). Some very low ΔE structural isomers (for example, isomer II of $^{3}FeVS^-$ ΔE = 0.06, first VDE = 0.61 eV) are not observed, although their calculated first VDEs are not overlapped with those of other isomers. These results suggest that the distributions/populations of structural isomers of Fe-V sulfur cluster anions can be generated either thermodynamically (through ΔE, ΔG) or kinetically (through transition state barriers). The obtained PES profile can provide an experimental method to assign coexisting structural isomers. Furthermore, electron distribution properties of the NBO/HOMO must also be an essential factor through which one can understand the first VDEs for Fe-V sulfur clusters compared to pure iron sulfur clusters. More comparison studies between larger Fe-V sulfur clusters and related pure iron sulfur clusters, with regard to how NBO/HOMO distributions affect their first VDEs, should certainly prove informative.

CONCLUSIONS

Iron-vanadium sulfur cluster anions are studied by PES at 3.492 eV (355 nm) and 4.661 eV (266 nm) photon energies, and by DFT calculations. The structural properties, relative energies of different structural isomers, and calculated first VDEs of different structural isomers for these cluster anions are investigated at BPW91/TZVP theory levels. The most probable structures and ground state spin multiplicities for these clusters are tentatively assigned by comparing their theoretical and experiment first VDE values.

The first VDEs for $FeVS_{1-3}^-$ clusters are generally observed to increase with the number of sulfur atoms from 1.5 eV to 2.8 eV. Diverse types of structural isomers are found for each $FeVS_x^-$ (x = 1 – 3) cluster. One type of structural isomer with a terminal sulfur bonded to a vanadium site (isomer I) is found for all $FeVS_{1-3}^-$ clusters: its calculated relative energy (ΔE) is obtained to be the lowest among all structural isomers for each species $FeVS_x^-$ (x = 1 – 3). The NBO/HOMOs of ground states (isomers I) of $FeVS_{1-3}^-$ clusters are localized in a *p* orbital on a S atom. The partial charge distribution on the NBO/HOMO localized sites of each cluster anion (considering the "charge effect") is probably responsible for the trend of their first VDEs. The "charge effect" on the NBO/HOMO localized site is suggested not to be an essential

factor that affects the first VDEs for three metal atoms containing Fe/V/S ($FeV_2S_3^-$ and $Fe_2VS_3^-$) clusters. With different Fe/V ratios for these clusters, the ground state structures are different: structure and steric effect differences are responsible for their different first VDEs and properties. Two types structural isomers are found for $Fe_mV_nS_{m+n}^-$ ($m + n = 4$, $m > 0$, $n > 0$) clusters: tower structure and cubic structure isomers. For the $FeV_3S_4^-$ cluster anion, only the tower structure isomer is observed. Both tower and cubic structure isomers are observed for $Fe_2V_2S_4^-$ and $Fe_3VS_4^-$ clusters. The metal ratio in these four metal atom containing Fe/V/S cluster anions is probably the main factor that affects the structure properties for these Fe/V/S clusters. The first VDEs for tower like isomers are generally higher than those for cubic like isomers of $Fe_mV_nS_{m+n}^-$ ($m + n = 4$, $m > 0$, $n > 0$) clusters. Their first VDEs are reported and suggested to be understood through: (1) NBO/HOMO distributions, (2) structures (steric effect), and (3) partial charge number on the NBO/HOMOs localized sites ("charge effect").

EBEs regarding excited state transitions for related Fe/V/S are calculated employing OVGF and TDDFT approaches at a TZVP basis set level. The OVGF approach is generally better for higher transition energy theoretical studies of Fe/V/S cluster anions. The experimental and theoretical results of these Fe/V/S cluster anions are compared with their related pure Fe/S cluster

anions. The electron distribution (wave function) properties of the NBO/HOMO are suggested to be an essential factor for understanding and comparing the different first VDEs of Fe/V/S cluster anions to those of pure Fe/S cluster anions.

Supporting Information. The following results are supplied as additional detailed information for these studies: 1. mass spectrum of $Fe_mV_nS_xC_y^-$ cluster anions generated by laser ablation of a mixed Fe:V = 1:1 target in the presence of a 0.1% CS_2 in He carrier gas is presented in Figure S1; 2. DFT optimized structures of $FeV_3S_4^-$ cluster at the BPW91/TZVP level is displayed in Figure S2; 3. NBO plots showing HOMO to HOMO-4 orbitals of $FeVS_{1-3}^-$ and $Fe_mV_nS_{m+n}^-$ ($m + n = 3, 4$; $m > 0$, $n > 0$) clusters are displayed in Figures S3 to S5; 4. brief description of broken symmetry; and 5. spin orbit coupling (SOC) corrected calculational results for $(FeS)_{1,2}^-$ clusters.

ACKNOWLEDGMENT

This work is supported by a grant from the US Air Force Office of Scientific Research (AFOSR) through grant number FA9550-10-1-0454, the National

Science Foundation (NSF) ERC for Extreme Ultraviolet Science and Technology under NSF Award No. 0310717, the Army Research Office (ARO, Grant Nos. FA9550-10-1-0454 and W911-NF13-10192), and a DoD DURIP grant (W911NF-13-1-0192).

REFERENCES

(1) Monosson, E., *Evolution in a Toxic World* (Island Press/Center for Resource Economics, 2012).
(2) Cammack, R., *Advances in Inorganic Chemistry* (Academic Press, New York, 1992), Vol. 38.
(3) Nurmaganbetova, M. S.;Baikenov, M. I.;Meiramov, M. G.;Mukhtar, A. A.;Ordabaeva, A. T.;Khrupov, V. A. Catalytic Hydrogenation of Anthracene on Modified Iron Sulfide Catalysts. *Pet. Chem.* **2001,** *41*, 26-29.
(4) Munck, E.;Bominaar, E. L. Chemistry - Bringing Stability to Highly Reduced Iron-Sulfur Clusters. *Science* **2008,** *321*, 1452-1453.
(5) Rees, D. C.;Howard, J. B. The Interface between the Biological and Inorganic Worlds: Iron-Sulfur Metalloclusters. *Science* **2003,** *300*, 929-931.
(6) Bryant, R. D.;Kloeke, F. V.;Laishley, E. J. Regulation of the Periplasmic Fe Hydrogenase by Ferrous Iron in Desulfovibrio-Vulgaris (Hildenborough). *Appl. Environ. Microbiol.* **1993,** *59*, 491-495.
(7) Holm, R. H.;Kennepohl, P.;Solomon, E. I. Structural and Functional Aspects of Metal Sites in Biology. *Chem Rev* **1996,** *96*, 2239-2314.
(8) Ogino, H.;Inomata, S.;Tobita, H. Abiological Iron−Sulfur Clusters. *Chem Rev* **1998,** *98*, 2093-2122.
(9) Koszinowski, K.;Schröder, D.;Schwarz, H. Formation and Reactivity of Gaseous Iron-Sulfur Clusters. *Eur J Inorg Chem* **2004,** *1*, 44-50.
(10) Koszinowski, K.;Schröder, D.;Schwarz, H.;Liyanage, R.;Armentrout, P. B. Thermochemistry of Small Cationic Iron-Sulfur Clusters. *J Chem Phys* **2002,** *117*, 10039-10056.
(11) Whetten, R. L.;Cox, D. M.;Trevor, D. J.;Kaldor, A. Free Iron Clusters React Readily with Oxygen and Hydrogen Sulfide, but Are Inert toward Methane. *J Phys Chem* **1985,** *89*, 566-569.
(12) Yin, S.;Wang, Z. C.;Bernstein, E. R. Formaldehyde and Methanol Formation from Reaction of Carbon Monoxide and Hydrogen on Neutral Fe_2S_2 Clusters in the Gas Phase. *Phys Chem Chem Phys* **2013,** *15*, 4699-4706.
(13) Zhai, H.-J.;Kiran, B.;Wang, L.-S. Electronic and Structural Evolution of Monoiron Sulfur Clusters, FeS_n^- and FeS_n (n = 1− 6), from Anion Photoelectron Spectroscopy. *J Phys. Chem. A* **2003,** *107*, 2821-2828.
(14) Nakajima, A.;Hayase, T.;Hayakawa, F.;Kaya, K. Study on Iron-Sulfur Cluster in Gas Phase: Electronic Structure and Reactivity. *Chem Phys Lett* **1997,** *280*, 381-389.

(15) Zhang, N.;Hayase, T.;Kawamata, H.;Nakao, K.;Nakajima, A.;Kaya, K. Photoelectron Spectroscopy of Iron-Sulfur Cluster Anions. *J Chem Phys* **1996,** *104*, 3413-3419.
(16) Fu, Y. J.;Yang, X.;Wang, X. B.;Wang, L. S. Probing the Electronic Structure of 2Fe-2S Clusters with Three Coordinate Iron Sites by Use of Photoelectron Spectroscopy. *J Phys Chem A* **2005,** *109*, 1815-1820.
(17) Fu, Y. J.;Laskin, J.;Wang, L. S. Electronic Structure and Fragmentation Properties of $[Fe_4S_4(SEt)_{4-x}(SSEt)_x]^{2-}$. *Int J Mass Spectrom* **2007,** *263*, 260-266.
(18) Fu, Y. J.; Laskin, J.; Wang, L. S., Collision-Induced Dissociation of [4Fe-4S] Cubane Cluster Complexes: $Fe_4S_4Cl_{4-x}(SC_2H_5)_x^{2-/1-}$ (x = 0-4). *Int. J. Mass Spectrom.* **2006,** *255*, 102-110.
(19) Yang, X.; Niu, S. Q.; Ichiye, T.; Wang, L. S., Direct measurement of the hydrogen-bonding effect on the intrinsic redox potentials of 4Fe-4S cubane complexes. *J. Am. Chem. Soc.* **2004,** *126*, 15790-15794.
(20) El Nakat, J.; Fisher, K. J.; Dance, I. G.; Willett, G. D., Gas Phase Metal Chalcogenide Cluster Ions: A New $[Co_xS_y]^-$ Series up to $[Co_{38}S_{24}]^-$ and Two Iron-Sulfur $[Fe_xS_y]^-$ Series. *Inorg. Chem.* **1993,** *32*, 1931-1940.
(21) Hubner, O.;Sauer, J. The Electronic States of $Fe_2S_2^{-/0/+/2+}$. *J Chem Phys* **2002,** *116*, 617-628.
(22) Hubner, O.;Sauer, J. Structure and Thermochemistry of $Fe_2S_2^{-/0/+}$ Gas Phase Clusters and Their Fragments. B3lyp Calculations. *Phys Chem Chem Phys* **2002,** *4*, 5234-5243.
(23) Ding, L.-P.;Kuang, X.-Y.;Shao, P.;Zhong, M.-M. Evolution of the Structure and Electronic Properties of Neutral and Anion FeS_n^{μ} (n=1-7, μ=0,-1) Clusters: A Comprehensive Analysis. *J Alloys Compd* **2013,** *573*, 133-141.
(24) Noodleman, L.;Peng, C. Y.;Case, D. A.;Mouesca, J. M. Orbital Interactions, Electron Delocalization and Spin Coupling in Iron-Sulfur Clusters. *Coord Chem Rev* **1995,** *144*, 199-244.
(25) Mouesca, J.-M.;Lamotte, B. Iron–Sulfur Clusters and Their Electronic and Magnetic Properties. *Coord Chem Rev* **1998,** *178–180, Part 2*, 1573-1614.
(26) Yin, S.;Bernstein, E. R. Photoelectron Spectroscopy and Density Functional Theory Studies of Iron Sulfur $(FeS)_m^-$ (m = 2–8) Cluster Anions: Coexisting Multiple Spin States. *J Phys Chem A* **2017,** *121*, 7362-7373.
(27) Chasteen, N. D., *Vanadium in Biological Systems* (Springer Netherlands, 1990).
(28) Michibata, H.;Yamaguchi, N.;Uyama, T.;Ueki, T. Molecular Biological Approaches to the Accumulation and Reduction of Vanadium by Ascidians. *Coord Chem Rev* **2003,** *237*, 41-51.
(29) Eady, R. R. Current Status of Structure Function Relationships of Vanadium Nitrogenase. *Coord Chem Rev* **2003,** *237*, 23-30.
(30) Hitoshi, M.;Taro, U.;Tatsuya, U.;Kan, K. Vanadocytes, Cells Hold the Key to Resolving the Highly Selective Accumulation and Reduction of Vanadium in Ascidians. *Microscopy Research and Technique* **2002,** *56*, 421-434.
(31) Dieter, R. The Bioinorganic Chemistry of Vanadium. *Angewandte Chemie International Edition in English* **1991,** *30*, 148-167.
(32) Crans, D. C.;Smee, J. J.;Gaidamauskas, E.;Yang, L. The Chemistry and Biochemistry of Vanadium and the Biological Activities Exerted by Vanadium Compounds. *Chem Rev* **2004,** *104*, 849-902.
(33) Rehder, D. Vanadium Nitrogenase. *Journal of Inorganic Biochemistry* **2000,** *80*, 133-136.
(34) Malinak, S. M.;Demadis, K. D.;Coucouvanis, D. Catalytic Reduction of Hydrazine to Ammonia by the VFe_3S_4 Cubanes. Further Evidence for the Direct Involvement of the

Heterometal in the Reduction of Nitrogenase Substrates and Possible Relevance to the Vanadium Nitrogenases. *J Am Chem Soc* **1995,** *117*, 3126-3133.
(35) Corderman, R.;Lineberger, W. Negative Ion Spectroscopy. *Annu Rev Phys Chem* **1979,** *30*, 347-378.
(36) Harvey, J. N., in *Principles and Applications of Density Functional Theory in Inorganic Chemistry I* (Springer Berlin Heidelberg, Berlin, Heidelberg, 2004), pp. 151-184.
(37) Yin, S.;Bernstein, E. R. Properties of Iron Sulfide, Hydrosulfide, and Mixed Sulfide/Hydrosulfide Cluster Anions through Photoelectron Spectroscopy and Density Functional Theory Calculations. *J Chem Phys* **2016,** *145*, 154302.
(38) Zeng, Z.;Bernstein, E. R. Photoelectron Spectroscopy and Density Functional Theory Studies of N-Rich Energetic Materials. *J Chem Phys* **2016,** *145*, 164302.
(39) Wu, H.;Desai, S. R.;Wang, L.-S. Chemical Bonding between Cu and Oxygen Copper Oxides vs O_2 Complexes: A Study of CuO_x (x = 0− 6) Species by Anion Photoelectron Spectroscopy. *J Phys. Chem. A* **1997,** *101*, 2103-2111.
(40) Frisch, M. J.;Trucks, G. W.;Schlegel, H. B.;Scuseria, G. E.;Robb, M. A.;Cheeseman, J. R.;Scalmani, G.;Barone, V.;Mennucci, B.;Petersson, G. A.;Nakatsuji, H.;Caricato, M.;Li, X.;Hratchian, H. P.;Izmaylov, A. F.;Bloino, J.;Zheng, G.;Sonnenberg, J. L.;Hada, M.;Ehara, M.;Toyota, K.;Fukuda, R.;Hasegawa, J.;Ishida, M.;Nakajima, T.;Honda, Y.;Kitao, O.;Nakai, H.;Vreven, T.;Montgomery Jr., J. A.;Peralta, J. E.;Ogliaro, F.;Bearpark, M. J.;Heyd, J.;Brothers, E. N.;Kudin, K. N.;Staroverov, V. N.;Kobayashi, R.;Normand, J.;Raghavachari, K.;Rendell, A. P.;Burant, J. C.;Iyengar, S. S.;Tomasi, J.;Cossi, M.;Rega, N.;Millam, N. J.;Klene, M.;Knox, J. E.;Cross, J. B.;Bakken, V.;Adamo, C.;Jaramillo, J.;Gomperts, R.;Stratmann, R. E.;Yazyev, O.;Austin, A. J.;Cammi, R.;Pomelli, C.;Ochterski, J. W.;Martin, R. L.;Morokuma, K.;Zakrzewski, V. G.;Voth, G. A.;Salvador, P.;Dannenberg, J. J.;Dapprich, S.;Daniels, A. D.;Farkas, Ö.;Foresman, J. B.;Ortiz, J. V.;Cioslowski, J.;Fox, D. J., Gaussian 09. Gaussian, Inc.: Wallingford, CT, USA, 2009.
(41) Noodleman, L.;Norman Jr, J. G.;Osborne, J. H.;Aizman, A.;Case, D. A. Models for Ferredoxins: Electronic Structures of Iron-Sulfur Clusters with One, Two, and Four Iron Atoms. *J Am Chem Soc* **1985,** *107*, 3418-3426.
(42) Anderson, R. E.; Dunham, W. R.; Sands, R. H.; Bearden, A. J.; Crespi, H. L. On the Nature of the Iron Sulfur Cluster in a Deuterated Algal Ferredoxin. *BBA-Bioenergetics* **1975,** *408*, 306-318.
(43) Hübner, O.; Sauer, J. The Electronic States of $Fe_2S_2^{-/0/+/2+}$. *J Chem. Phys.* **2002,** *116*, 617-628.
(44) Perdew, J. P.;Wang, Y. Accurate and Simple Analytic Representation of the Electron-Gas Correlation-Energy. *Phys Rev B* **1992,** *45*, 13244-13249.
(45) Weigend, F.;Ahlrichs, R. Balanced Basis Sets of Split Valence, Triple Zeta Valence and Quadruple Zeta Valence Quality for H to Rn: Design and Assessment of Accuracy. *Phys Chem Chem Phys* **2005,** *7*, 3297-3305.
(46) Yin, S.;Xie, Y.;Bernstein, E. R. Hydrogenation Reactions of Ethylene on Neutral Vanadium Sulfide Clusters: Experimental and Theoretical Studies. *J Phys Chem A* **2011,** *115*, 10266-10275.
(47) Becke, A. D. Density-Functional Thermochemistry 3. The Role of Exact Exchange. *J Chem Phys* **1993,** *98*, 5648-5652.
(48) Lee, C. T.;Yang, W. T.;Parr, R. G. Development of the Colle-Salvetti Correlation-Energy Formula into a Functional of the Electron-Density. *Phys Rev B* **1988,** *37*, 785-789.

(49) Becke, A. D. Density-Functional Exchange-Energy Approximation with Correct Asymptotic Behavior. *Phys Rev A* **1988,** *38*, 3098-3100.
(50) Perdew, J. P.;Burke, K.;Wang, Y. Generalized Gradient Approximation for the Exchange-Correlation Hole of a Many-Electron System. *Phys Rev B* **1996,** *54*, 16533-16539.
(51) Austin, A.;Petersson, G. A.;Frisch, M. J.;Dobek, F. J.;Scalmani, G.;Throssell, K. A Density Functional with Spherical Atom Dispersion Terms. *J. Chem. Theory Comput.* **2012,** *8*, 4989-5007.
(52) Rassolov, V. A.;Pople, J. A.;Ratner, M. A.;Windus, T. L. 6-31g* Basis Set for Atoms K through Zn. *J Chem Phys* **1998,** *109*, 1223-1229.
(53) Krishnan, R.; Binkley, J. S.; Seeger, R.; Pople, J. A. Self-Consistent Molecular Orbital Methods. XX. A Basis Set for Correlated Wave Functions. *J Chem. Phys.* **1980,** *72*, 650-654.
(54) Hehre, W. J.; Ditchfield, R.; Pople, J. A. Self-Consistent Molecular Orbital Methods. Xii. Further Extensions of Gaussian Type Basis Sets for Use in Molecular Orbital Studies of Organic Molecules. *J Chem. Phys.* **1972,** *56*, 2257-2261.
(55) Dunning, T. H. Gaussian Basis Sets for Use in Correlated Molecular Calculations. I. The Atoms Boron through Neon and Hydrogen. *J Chem Phys* **1989,** *90*, 1007-1023.
(56) Casida, M. E.;Jamorski, C.;Casida, K. C.;Salahub, D. R. Molecular Excitation Energies to High-Lying Bound States from Time-Dependent Density-Functional Response Theory: Characterization and Correction of the Time-Dependent Local Density Approximation Ionization Threshold. *J Chem Phys* **1998,** *108*, 4439-4449.
(57) Cederbaum, L. One-Body Green's Function for Atoms and Molecules: Theory and Application. *J Phys. B At. Mol. Opt. Phys.* **1975,** *8*, 290.
(58) Hunt, P. A.; Kirchner, B.; Welton, T. Characterising the Electronic Structure of Ionic Liquids: An Examination of the 1-Butyl-3-Methylimidazolium Chloride Ion Pair. *Chem. Eur. J* **2006,** *12*, 6762-6775.
(59) Siegbahn, K., *Esca Applied to Free Molecules* (North-Holland, Amsterdam, 1969).
(60) Yin, S.;Bernstein, E. R. Photoelectron Spectroscopy and Density Functional Theory Studies of $(FeS)_mH^-$ (m = 2-4) Cluster Anions: Effects of the Single Hydrogen. *Phys. Chem. Chem. Phys.* **2018,** *20*, 367-382.

Figures and Tables

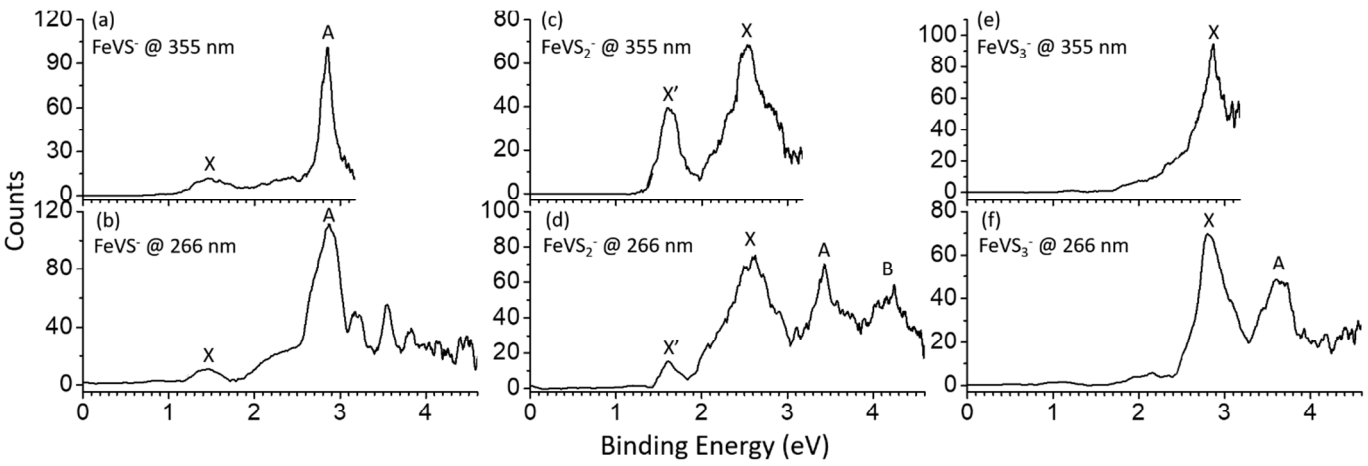

Figure 1. Photoelectron spectra of $FeVS_{1\text{-}3}^-$ cluster anions at 355 nm and 266 nm. X and X' label the ground state transition peaks, and A and B label the first and second low-lying transition peaks at high VDE (see assignment details presented in Table I).

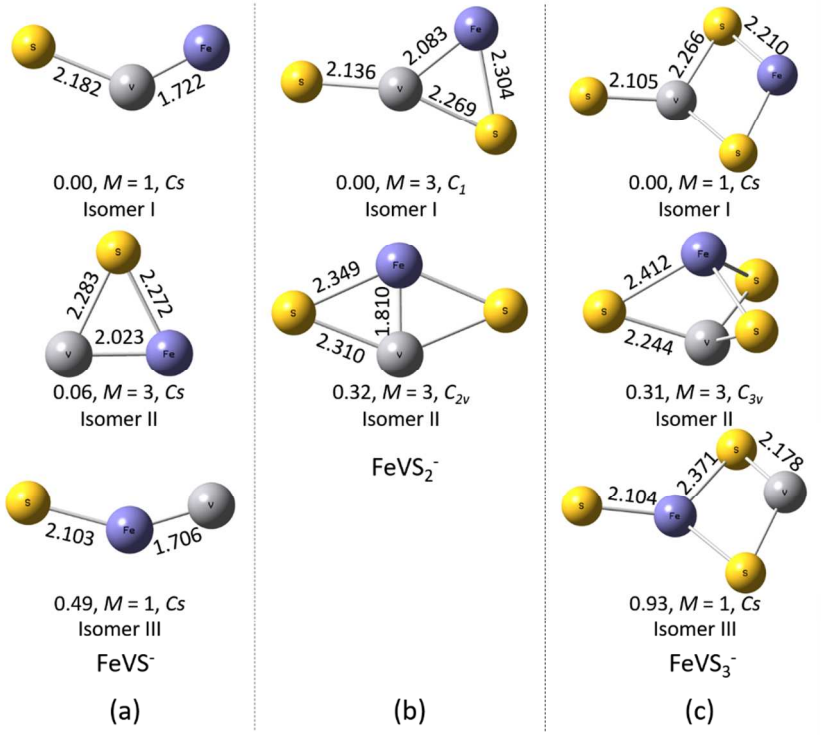

Figure 2. DFT optimized structures of (a) $FeVS^-$ (b) $FeVS_2^-$ and (c) $FeVS_3^-$ clusters at the BPW91/TZVP level. The lowest relative energy spin state geometry of each isomer is displayed in this figure. Geometries of other spin states for each cluster are generally similar to the one shown but with slightly different bond lengths and angles. Bond lengths (in angstroms), relative energy (in eV), spin multiplicity *M*, and point group symmetry are indicated on the structures. [Grey = V, blue = Fe, yellow = S]

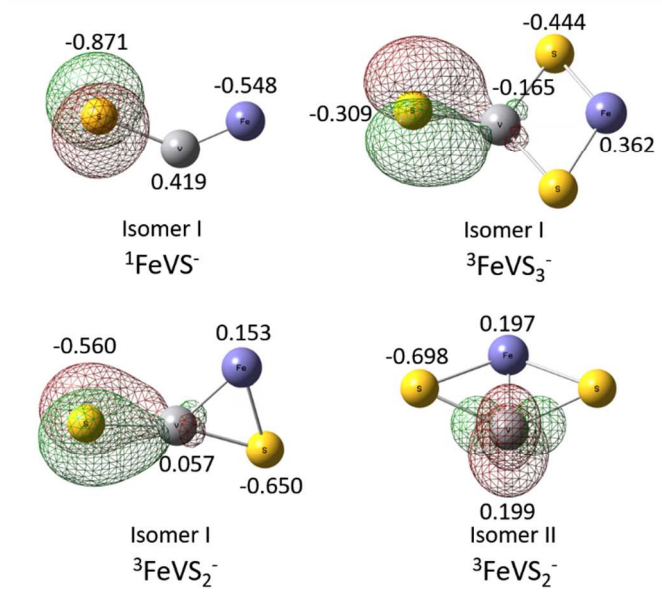

Figure 3. NBO plots showing the highest occupied molecular orbital (HOMO) of $FeVS_{1-3}^{-}$ cluster anions. The spin multiplicity (*M*) is listed as $^{M}FeVS_{1-3}^{-}$. The NBO charges for important atoms are given in the Figure. [Grey = V, blue = Fe, yellow = S]

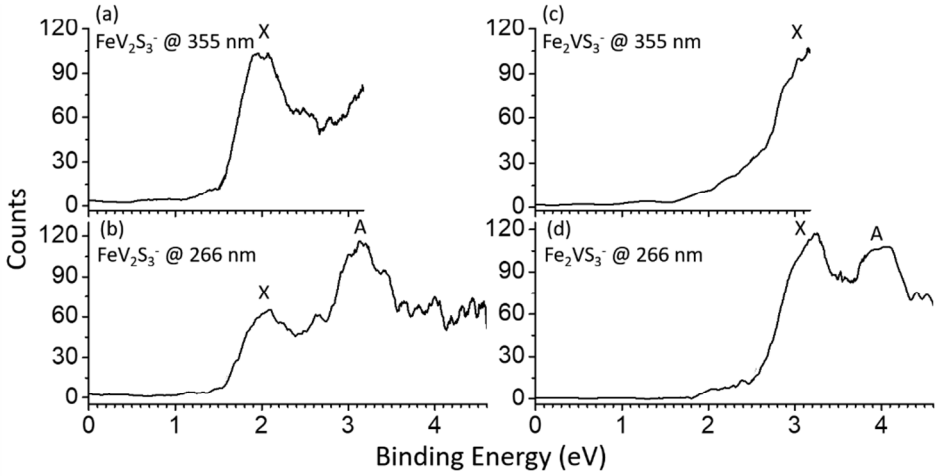

Figure 4. Photoelectron spectra of $FeV_2S_3^-$ and $Fe_2VS_3^-$ cluster anions at 355 nm and 266 nm. X label the ground state transition peak, and A labels the first low-lying transition peak at high VDE (see assignment details presented in Table II).

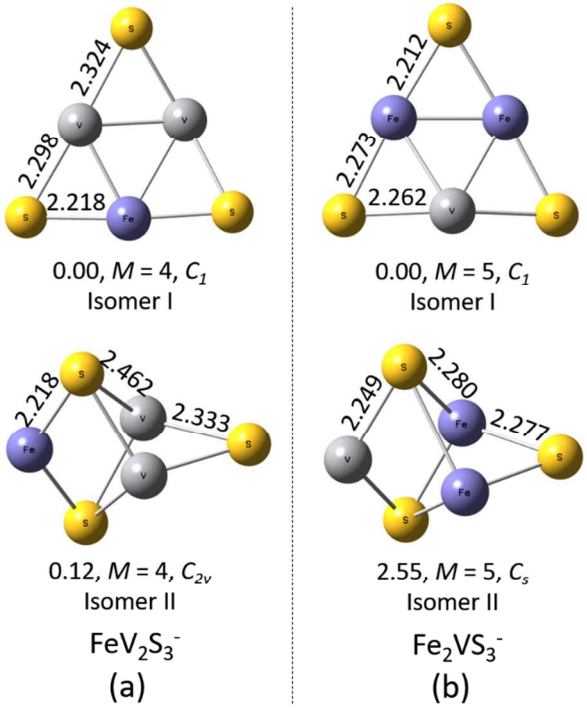

Figure 5. DFT optimized structures of (a) $FeV_2S_3^-$ and (b) $Fe_2VS_3^-$ at the BPW91/TZVP level. The lowest relative energy spin state geometry of each isomer is displayed in this figure. Geometries of other spin states for each cluster are generally similar to the one shown but with slightly different bond lengths and angles. Bond lengths (in angstroms), relative energy (in eV), spin multiplicity *M*, and point group symmetry are indicated on the structures. [Grey = V, blue = Fe, yellow = S]

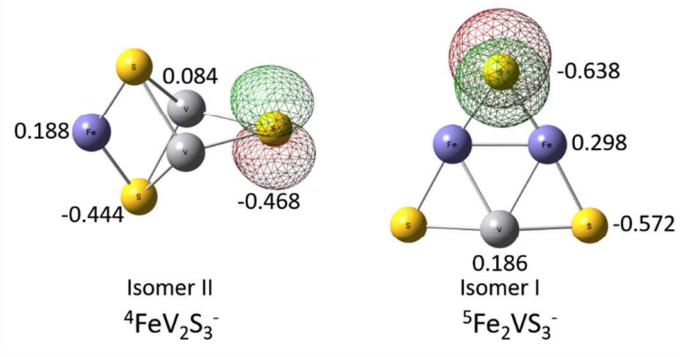

Figure 6. NBO plots showing the highest occupied molecular orbital (HOMO) of $FeV_2S_3^-$ and $Fe_2VS_3^-$ cluster anions. The spin multiplicity (M) is listed as $^{M}Fe_mV_nS_{m+n}^-$. The NBO charges for important atoms are given in the Figure. [Grey = V, blue = Fe, yellow = S]

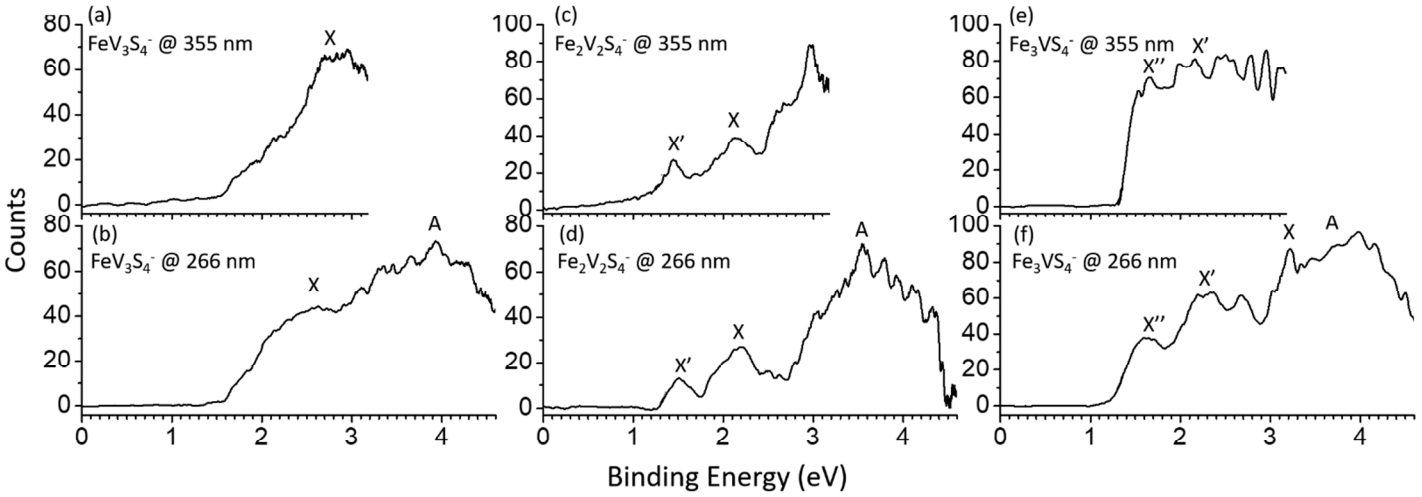

Figure 7. Photoelectron spectra of $Fe_mV_nS_{m+n}^-$ ($m + n = 4$, $m > 0$, $n > 0$) cluster anions at 355 nm and 266 nm. X, X' and X'' label the ground state transition peaks, and A and B label the first and second low-lying transition peaks at high VDE (see assignment details presented in Table III).

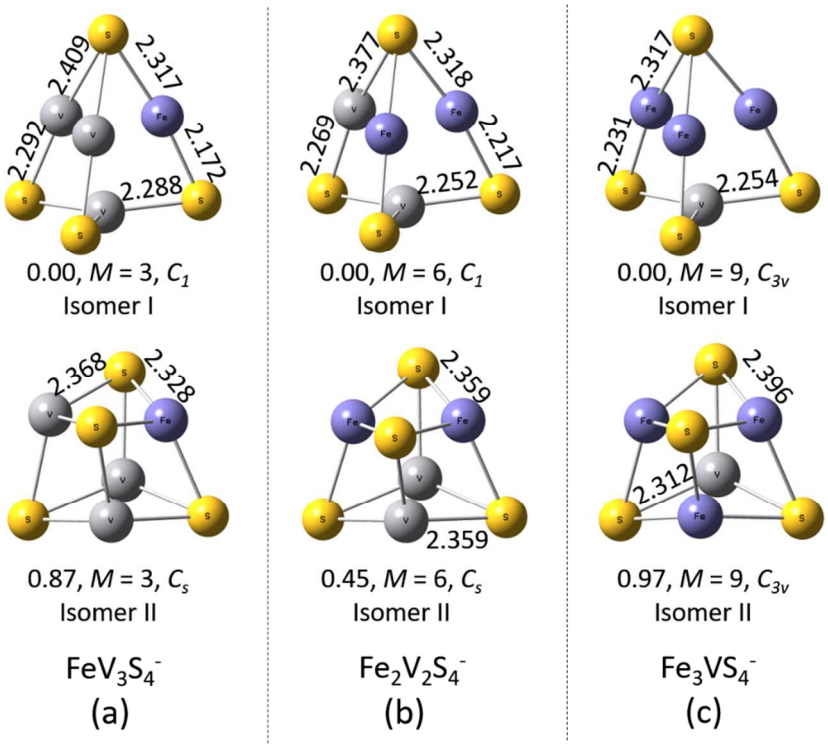

Figure 8. DFT optimized structures of (a) $FeV_3S_4^-$ (b) $Fe_2V_2S_4^-$ and (c) $Fe_3VS_4^-$ clusters at the BPW91/TZVP level. The lowest relative energy spin state geometry of each isomer is displayed in this figure. Geometries of other spin states for each cluster are generally similar to the one shown but with slightly different bond lengths and angles. Bond lengths (in angstroms), relative energy (in eV), spin multiplicity *M*, and point group symmetry are indicated on the structures. [Grey = V, blue = Fe, yellow = S]

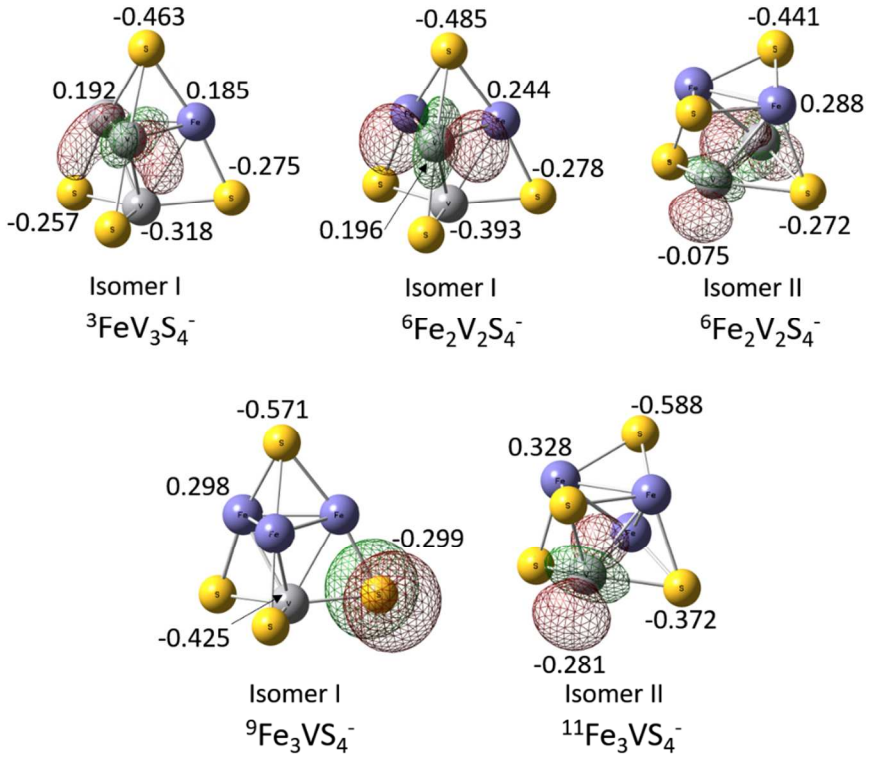

Figure 9. NBO plots showing the highest occupied molecular orbital (HOMO) of $Fe_mV_nS_{m+n}^-$ ($m + n = 4$, $m > 0$, $n > 0$) cluster anions. The spin multiplicity (M) is listed as $^{M}Fe_mV_nS_{m+n}^-$. The NBO charges for important atoms are given in the Figure. [Grey = V, blue = Fe, yellow = S]

Table I. The calculated VDEs (in eV) for $FeVS_{1-3}^-$ clusters at BPW91/TZVP level, as well as the experimental results for comparison. Following EBE values after the first VDE are calculated employing TDDFT at the BPW91/TZVP level and the OVGF/TZVP method. The relative energy (ΔE) of different isomers with their various spin multiplicities are presented for each cluster (ΔGs are given in the brackets).

Cluster	Structural isomer	Spin (*M=2S+1*)	BPW91/TZVP (eV)		Exp.	
			ΔE	Calculated VDE	Observed feature	VDE
$FeVS^-$	Isomer I	1	0.00 (0.00)	1.82 [a]	X	1.45
				3.22 [b] 2.17 [c]	A	2.85
	Isomer II	3	0.06 (0.03)	0.61 [a]	Not observed	
	Isomer III	1	0.49 (0.50)	1.61 [a]	X	1.45
				2.52 [b] 2.45 [c]	A	2.85
$FeVS_2^-$	Isomer I	3	0.00 (0.00)	2.46 [a]	X	2.55
				3.46 [b] 3.13 [c]	A	3.45
				3.94 [b] --	B	4.20
	Isomer II	3	0.32 (0.39)	1.76 [a]	X'	1.63
				3.42 [b] 2.08 [c]	A	3.45
				4.07 [b] --	B	4.20
$FeVS_3^-$	Isomer I	3	0.00 (0.00)	2.46 [a]	X	2.86
				4.43 [b] 2.86 [c]	A	3.65
	Isomer II	3	0.31 (0.33)	2.87 [a]	X	2.86
				3.81 [b] 3.88 [c]	A	3.65
	Isomer III	3	0.93 (0.89)	2.76 [a]	X	2.86
				3.91 [b] 3.16 [c]	A	3.65

[a] The calculated first VDE.
[b] The calculated following EBE value after the first VDE employing the OVGF/TZVP method.
[c] The calculated following EBE value after the first VDE employing TDDFT at the BPW91/TZVP level.

Table II. The calculated VDEs (in eV) for $FeV_2S_3^-$ and $Fe_2VS_3^-$ clusters at BPW91/TZVP level, as well as the experimental results for comparison. Following EBE values after the first VDE are calculated employing TDDFT at the BPW91/TZVP level and the OVGF/TZVP method. The relative energy (ΔE) of different isomers with their various spin multiplicities are presented for each cluster (ΔGs are given in the brackets).

Cluster	Structural isomer	Spin (*M=2S+1*)	BPW91/TZVP (eV)		Exp.	
			ΔE	Calculated VDE	Observed feature	VDE
$FeV_2S_3^-$	Isomer I	4	0.00 (0.00)	2.55 [a]	X	2.00
				4.13 [b] 2.90 [c]	A	3.17
	Isomer II	4	0.12 (0.16)	2.22 [a]	X	2.00
				3.77 [b] 3.02 [c]	A	3.17
$Fe_2VS_3^-$	Isomer I	5	0.00 (0.00)	2.58 [a]	X	3.18
				4.17 [b] 3.15 [c]	A	~ 4.0
	Isomer II	5	2.55 (2.60)	1.31 [a]	Not observed	

[a] The calculated first VDE.
[b] The calculated following EBE value after the first VDE employing the OVGF/TZVP method.
[c] The calculated following EBE value after the first VDE employing TDDFT at the BPW91/TZVP level.

Table III. The calculated VDEs (in eV) for $Fe_mV_nS_{m+n}^-$ ($m + n = 4$, $m > 0$, $n > 0$) clusters at BPW91/TZVP level, as well as the experimental results for comparison. Following EBE values after the first VDE are calculated employing TDDFT at the BPW91/TZVP level and the OVGF/TZVP method. The relative energy (ΔE) of different isomers with their various spin multiplicities are presented for each cluster (ΔGs are given in the brackets).

Cluster	Structural isomer	Spin (*M=2S+1*)	BPW91/TZVP (eV)		Exp.	
			ΔE	Calculated VDE	Observed feature	VDE
$FeV_3S_4^-$	Isomer I	3	0.00 (0.00)	2.64 [a]	X	~ 2.7
				3.89 [b] 3.15 [c]	A	~ 4.0
	Isomer II	3	0.87 (0.88)	1.28 [a]	Not observed	
$Fe_2V_2S_4^-$	Isomer I	4	0.00 (0.02)	2.39 [a]	X	2.17
				4.47 [b] 3.15 [c]	A	~ 3.5
		6	0.00 (0.00)	2.31 [a]	X	2.17
				3.82 [b] 3.14 [c]	A	~ 3.5
	Isomer II	6	0.45 (0.48)	1.46 [a]	X'	1.50
				3.93 [b] 1.86 [c]	A	~ 3.5
		8	0.40 (0.44)	1.49 [a]	X'	1.50
				3.77 [b] 1.91 [c]	A	~ 3.5
$Fe_3VS_4^-$	Isomer I	9	0.00 (0.00)	3.19 [a]	X	3.20
				4.76 [b] 3.75 [c]	A	3. 5 – 4.4
		11	0.72 (0.70)	2.32 [a]	X'	2.30
				4.53 [b] 2.76 [c]	A	3. 5 – 4.4
	Isomer II	9	0.97 (0.97)	1.70 [a]	X''	1.60
				4.26 [b] 2.62 [c]	A	3. 5 – 4.4
		11	0.87 (0.88)	1.88 [a]	X''	1.60
				4.00 [b] 2.79 [c]	A	3. 5 – 4.4

[a] The calculated first VDE.
[b] The calculated following EBE value after the first VDE employing the OVGF/TZVP method.
[c] The calculated following EBE value after the first VDE employing TDDFT at the BPW91/TZVP level.